

## Performance of the SiPMs and Beta ASIC in the FIT Scintillating Fiber Tracker

**Keerthana Rajan Lathika,<sup>a,\*</sup> Giulio Lucchetta,<sup>a</sup> Javier Rico,<sup>a</sup> Juan Boix,<sup>a</sup> Laia Cardiel Sas,<sup>a</sup> Manel Martinez,<sup>a</sup> Oscar Blanch,<sup>a</sup> Chiara Perrina,<sup>b</sup> Jennifer Maria Frieden,<sup>b</sup> Kimberly Sarah Keyser,<sup>b</sup> Philipp Azzarello,<sup>c</sup> Albert Espinya,<sup>d</sup> Andreu Sanuy,<sup>d</sup> Daniel Guberman,<sup>d</sup> David Gascon,<sup>d</sup> Joan Mauricio<sup>d</sup> and Marina Orta<sup>d</sup>**

<sup>a</sup>*Institut de Física d'Altes Energies (IFAE), The Barcelona Institute of Science and Technology (BIST), E-08193 Bellaterra, Barcelona, Spain*

<sup>b</sup>*Institute of Physics, École Polytechnique Fédérale de Lausanne (EPFL), PH Building, Station 3, CH-1015 Lausanne, Switzerland*

<sup>c</sup>*Department of Nuclear and Corpuscular Physics (DPNC), University of Geneva, 24 quai Ernest-Ansermet, CH-1211 Geneva 4, Switzerland*

<sup>d</sup>*ICCUB, Department of Física Quàntica i Astrofísica, Institut de Ciències del Cosmos, Universitat de Barcelona, E-08007 Barcelona, Spain*

E-mail: [klathika@ifae.es](mailto:klathika@ifae.es)

The scintillating Fiber Tracker (FIT) has been designed as a tracking detector for the upcoming High Energy cosmic-Radiation Detection (HERD) facility. The FIT combines excellent angular resolution with precise charge reconstruction measurements for cosmic-ray detection. The tracker consists of multiple tracking planes made of fiber mats, arranged in two orthogonal directions, and read out with Hamamatsu S13552-10 SiPM arrays. A custom-made ASIC, the BETA ASIC, has been developed to fulfill the stringent requirements for noise, linearity, dynamic range, and power consumption of space applications. This work reports the performance of the SiPMs and the BETA read-out system used in FIT. Our setup has been optimized, characterized, and calibrated using an LED light source. Additionally, we discuss the system's performance in generating efficient triggers for the identification of ionizing particles.

39th International Cosmic Ray Conference (ICRC2025)  
15–24 July 2025  
Geneva, Switzerland



---

\*Speaker

## 1. Introduction

The precise measurement of charged particle trajectories is a fundamental requirement for cosmic-ray and gamma-ray experiments in space. Silicon strip tracker systems, such as those employed in the Fermi Large Area Telescope (Fermi-LAT), have long been the standard in this domain [1]. These detectors, typically constructed from multiple layers of silicon microstrip sensors combined with tungsten converters, deliver excellent spatial resolution and benefit from a high technology readiness level acquired through decades of research and operational experience in the space environment.

Despite their proven performance, silicon-based trackers present challenges for next-generation and large-scale missions, particularly due to their considerable mass, power consumption, and production cost. These factors can limit the achievable geometrical acceptance or the scalability of instruments intended for long-duration space operations.

Scintillating fiber trackers have emerged as a promising alternative, offering several key advantages. Utilizing thin plastic fibers that emit prompt scintillation light when traversed by charged particles, these systems can deliver spatial resolution comparable to that of silicon trackers. Direct readout using silicon photomultipliers (SiPMs) allows for fast signal response, reduced detector mass, and simplified, cost-effective fabrication. While their current technology readiness is somewhat lower than that of silicon-based solutions, rapid developments in photodetectors and readout electronics are driving their adoption in upcoming missions, such as HERD, NUSES, and ADAPT. As a result, scintillating fiber trackers are expected to play a major role in the next generation of space-based astroparticle experiments.

## 2. FIT Tracker and Readout System

The scintillating-fiber tracker (FIT) [2] has been developed as a modular, high-precision tracking detector to address the demands of future space missions. FIT is designed to accurately reconstruct the paths of charged particles, provide redundant measurements of the absolute electric charge, and facilitate gamma-ray conversion through electron-positron pair production. These capabilities are crucial for advancing cosmic-ray and gamma-ray astrophysics from space.

The FIT system features a scalable, sector-based architecture engineered for both comprehensive acceptance and high redundancy. Within every plane, multiple FIT modules—the fundamental building blocks of the tracker—are systematically arranged in two orthogonal orientations (X and Y) to provide true two-dimensional coordinate measurement.

Each module incorporates a single fiber mat constructed from six tightly packed layers of Kuraray SCSF-78MJ scintillating fibers, with each fiber having a diameter of  $250\text{ }\mu\text{m}$ . The fine fiber pitch and the charge-sharing effect between neighboring fibers allow the system to achieve spatial resolutions significantly better than the fiber diameter—typically around  $50\text{ }\mu\text{m}$ . The width of each mat is matched to the SiPM arrays to ensure efficient optical coupling and minimal light loss. Modules are mounted onto lightweight, rigid trays composed of carbon fiber reinforced polymer (CFRP) with an aluminum honeycomb core, combining mechanical stability with minimal mass—an essential feature for space-based instrumentation.

The scintillation light generated in the fiber mats is read out at each end by custom SiPM arrays developed for high-efficiency photon detection. The Hamamatsu S13552-10 arrays used in FIT each contain 128 SiPMs, with every SiPM comprising 3,749 pixels (arranged in a  $23 \times 163$  matrix) and a pixel pitch of  $10 \mu\text{m}$ . The high number of cells in each SiPM translates into a high dynamic range, allowing, in principle, the identification of particles up to iron. Each SiPM array is mounted on a dedicated printed circuit board equipped with integrated temperature sensors, allowing for real-time bias adjustment and gain stabilization. This design guarantees reliable performance and signal stability even under varying environmental conditions.

The readout of each SiPM channel in FIT is handled by the BETA ASIC [3], developed for precise, low-noise, and ultra-low-power operation in space environments. The version for the FIT is *BETA64*; *BETA16* is a preliminary 16-channel version that has been used for the tests so far. This chip supports 32 programmable gain configurations—split equally between high-gain and low-gain modes—enabling a wide dynamic range that extends from single photoelectron signals up to those produced by heavy ions, with automatic gain switching to prevent saturation and preserve measurement fidelity. Upon detecting light, the SiPM generates a current pulse that is immediately amplified and converted to voltage by the BETA preamplifier, which dynamically selects the appropriate gain path based on signal amplitude. The resulting voltage signal is then passed through a low-pass filter to reduce noise and allow reliable switching, followed by a shaping stage that produces a well-defined pulse with a predictable peak. This peak is captured by a track-and-hold circuit, after which the signal is digitized with an integrated Wilkinson analog-to-digital converter (ADC). Finally, the digitized data are transmitted via serial links for subsequent event building, calibration, and analysis, ensuring high precision and reliability throughout the entire readout chain.

The combination of FIT’s hierarchical sector-plane-module layout, dense fiber mats, high-granularity SiPM arrays, and advanced ASIC readout results in a powerful and flexible tracking system, purpose-built for the challenges of space-based astroparticle research. The following sections present the laboratory characterization and calibration of the FIT readout chain, with particular emphasis on the performance of the SiPMs and the BETA ASIC.

### 3. Experimental Setup

All laboratory measurements were carried out using a dedicated optical bench, with the entire setup placed inside a light-tight dark box (see Figure 1, left) to eliminate background contamination from ambient light and ensure that only controlled LED pulses are detected. Inside the dark box, three SiPM arrays are each read out by a stack of twenty BETA-16 ASIC mezzanines, allowing for the simultaneous and detailed characterization of a large number of channels. A pulsed LED light source provides accurate and reproducible illumination for testing and calibration, while a custom-designed slit mask—featuring narrow, precisely aligned slits—allows selective illumination of specific groups of SiPM channels. This configuration enables systematic studies of individual channel response and crosstalk under well-controlled conditions, forming a robust foundation for detailed performance analysis of the readout system.

Signal processing is managed externally by a front-end motherboard interfaced with a Xilinx FPGA (see Figure 1, right). This board handles data acquisition, configuration of the BETA ASICs,

and synchronization with the LED pulsing system. The FPGA enables fast and flexible readout, offering complete control over ASIC operation and allowing efficient accumulation of large datasets for detailed calibration and performance analysis. The FPGA also produces a trigger signal based on the logical combination of the individual pre-trigger signals produced by each BETA ASIC.

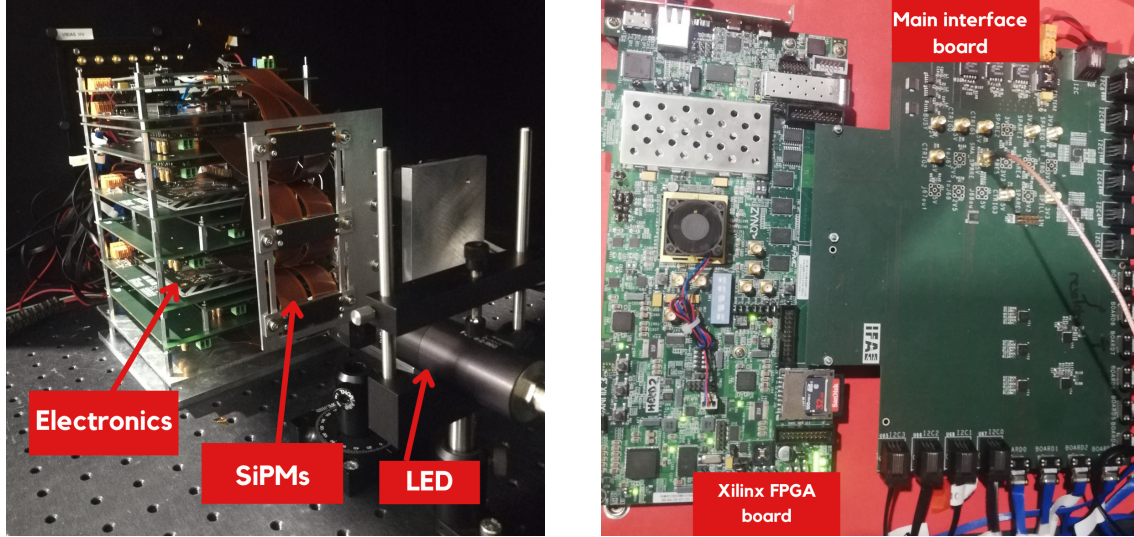


**Figure 1:** Experimental setup for FIT tracker readout characterization. On the left: dark box housing BETA-16 ASIC mezzanines, SiPM arrays, and LED source. On the right: front-end motherboard with Xilinx FPGA interface.

#### 4. Readout Configuration and Sampling Delay Optimization

The BETA ASIC features a number of internal parameters that must be carefully tuned to ensure accurate and stable readout of SiPM signals. Among these, the sampling delay is particularly important, as it determines the precise instant at which the SiPM output is digitized after a trigger. Setting this parameter correctly is essential, as sampling too early or too late lowers the signal-to-noise ratio and compromises the measurement quality.

To optimize the sampling delay, we begin by fixing the LED intensity and selecting the highest gain setting to enhance sensitivity. Next, we systematically scan the internal delay parameter of the BETA ASIC, which determines when the SiPM output is sampled after the trigger. For each delay setting, we record the average ADC response. As the sampling point approaches the pulse maximum, the measured signal increases, reaches a clear peak when perfectly aligned, and then decreases if sampled too late. The optimal delay is therefore chosen at the point where the signal is strongest, ensuring that all subsequent digitization captures the true pulse maximum for accurate and reliable measurements.

#### 5. Trigger Threshold Calibration

For each SiPM channel, the trigger threshold must be calibrated to reliably distinguish genuine photoelectron signals from electronic noise. In the BETA ASIC chip, each channel includes a

comparator that generates a trigger whenever the amplified SiPM output crosses a user-defined threshold. These thresholds are individually adjustable, enabling precise tuning for optimal sensitivity across all channels. A global asic pre-trigger signal is formed by the logical OR of the individual chip channel triggers.

The calibration procedure is performed under dark conditions, where no LED pulses are applied and only the intrinsic SiPM dark counts contribute to the signal. We systematically increase the threshold setting and record the trigger rate produced at each step. The resulting trigger rate curve exhibits a characteristic step-like pattern [4]: the count rate drops sharply each time the threshold crosses an integer multiple of the single-photoelectron signal. This structure is closely related to the dark count spectrum of the SiPM, which often shows a triple-peak shape due to random sampling of the bipolar shaper response—the central peak arises from electronic noise, while the two side peaks originate from randomly timed single-photoelectron pulses being sampled on the positive and negative lobes of the bipolar shaper.

To accurately locate the threshold values corresponding to each photoelectron level, we analyze the second derivative of the trigger rate curve. These threshold values are identified at the inflection points where the curve changes most rapidly. Setting the trigger thresholds at these points ensures high efficiency for real photon events while minimizing false triggers from noise, thereby providing a robust foundation for low-level signal detection and subsequent calibration.

## 6. SiPM Gain Calibration

Converting the digitized output from each SiPM channel into an accurate photon count is fundamental for achieving precise and reliable event reconstruction. This process requires establishing an accurate reference baseline, extracting the channel gain using well-resolved photon peaks, and extending calibration across all amplifier settings. Our calibration approach is designed to ensure both channel-by-channel accuracy and stability across the system's wide dynamic range, with a careful propagation of uncertainties throughout.

### 6.1 Pedestal Determination under Dark Conditions

SiPMs are operated with no light input, so recorded signals originate solely from electronic baseline fluctuations and inherent dark pulses. The resulting ADC histogram features a central baseline peak with smaller side lobes. The baseline level  $ADC_0$  is extracted using either the histogram peak or mean, which are equivalent for the symmetric SiPM dark-count distribution, differing by less than 0.1%, and subtracted from all subsequent measurements to establish a stable reference.

### 6.2 Absolute Gain Calibration

Controlled LED pulses are used to illuminate the SiPM at its highest amplifier gain, with the intensity varied to span the usable ADC dynamic range in this setting. The resulting ADC spectrum exhibits a sequence of well-separated peaks, each corresponding to a discrete number of detected photoelectrons. To maximize statistical precision and enhance the visibility of these peaks, data collected at different LED intensities are combined into a single, joint distribution.

A peak-finding algorithm is applied to the joint ADC spectrum to identify a photon peak at  $ADC_n$ —the ADC count corresponding to  $n$  photoelectrons, alongside the previously determined baseline  $ADC_0$ . Importantly, the calibration peak is selected to fall within the linear and unsaturated region of the ADC range—to ensure accurate gain measurement.

The absolute gain, in ADC counts per photon, is computed as:

$$C = \frac{ADC_n - ADC_0}{n} \quad [\text{counts per photon}],$$

where  $n$  is the number of photoelectrons corresponding to the chosen peak. To quantify the statistical uncertainty on  $C$ , an Asimov simulation is performed: synthetic histograms are generated by applying Poisson fluctuations to the observed data, the calibration is recalculated for each replica, and the standard deviation of the resulting distribution of calibration factors provides an estimator of the uncertainty  $\delta C$ .

This approach ensures a robust and precise determination of the absolute gain, establishing a reliable foundation for all subsequent calibration steps.

### 6.3 Relative Calibration Across Gain Settings

When operating at lower amplifier gains, individual photon peaks cannot be resolved. To maintain accurate calibration across these ranges, we use a relative calibration method. At a constant LED illumination level, we compare the pedestal-subtracted average signals between sequential gain settings. This comparison provides a conversion factor that links adjacent amplifier stages, ensuring consistent calibration throughout the dynamic range.

Concretely, for two consecutive gain levels  $i-1$  and  $i$ , the calibration factor  $C_i$  is derived from:

$$C_i = C_{i-1} \cdot \frac{S_i}{S_{i-1}},$$

where  $S_{i-1}$  and  $S_i$  are the mean LED response signals at their respective gains, after subtracting the baseline. This stepwise propagation builds upon the absolute gain determined at high gain, extending it seamlessly into lower-gain regions.

By repeating this process across all 32 gain configurations of the BETA-16 ASIC, from the most sensitive to the most robust, we cover the full signal range. The highest gain setting resolves up to 25 photoelectrons before saturation, while the lowest gain setting supports signals up to 8000 photoelectrons—sufficient for detecting high-charge nuclei up to iron (Fe), assuming that a minimum-ionizing particle generates about 10 photoelectrons.

### 6.4 Uniformity and Uncertainty Across Channels and ASICs

For each ASIC we analyze its three most-illuminated channels. At every gain setting  $i$  the average calibration factor is

$$\bar{C}_i = \frac{1}{3} \sum_{j=1}^3 C_i^{(j)}.$$

We then compute two key uncertainties:

- **Statistical uncertainty**  $\sigma_{\text{stat}}(i) = \frac{1}{N^2} \sqrt{\sum_{j=1}^N [\delta C_i^{(j)}]^2}$ ,
- **Dispersion uncertainty**  $\sigma_{\text{disp}}(i) = \sqrt{\frac{1}{N-1} \sum_{j=1}^N [C_i^{(j)} - \bar{C}_i]^2}$ .

where

- $N$  is the number of reference channels per ASIC and gain (three in this case); is
- $\delta C_i^{(j)}$  is the statistical error from Asimov-simulation based uncertainty for channel  $j$ ; right
- $\bar{C}_i$  denotes the average calibration factor across the reference channels;

We consistently find that  $\sigma_{\text{disp}}(i)$  exceeds  $\sigma_{\text{stat}}(i)$ . This indicates that the main uncertainty comes from differences between channels rather than from statistical noise. Using the average  $\bar{C}_i$  of the three reference channels and propagating both dispersion and statistical terms, we derive calibration constants for all 32 gain settings of each ASIC. The resulting gain table is precise and stable across the full dynamic range, ensuring reliable and reproducible signal reconstruction in all future data analyses.

## 7. Automatic Gain Switching Optimization

The BETA-16 ASIC is designed to handle both weak and strong signals by automatically switching between two amplification modes: high gain, which gives detailed measurements for small signals, and low gain, which prevents strong signals from exceeding the system's measurement limits. For this mechanism to work optimally, it is necessary to precisely set the point at which the switch from high to low gain occurs.

To establish this switching point, the system is first calibrated so that the number of detected photoelectrons can be related to the digitized output. Using this calibration, we determine the output value that corresponds to a chosen threshold—typically, a value halfway between the signals produced by minimum ionizing particles (MIPs, around 10 photoelectrons) and those from heavier nuclei such as helium (around 40 photoelectrons). The optimal threshold is set to about 20 photoelectrons, ensuring that MIP signals are always measured in high-gain mode, while larger signals are redirected to low gain before any risk of measurement overflow.

The actual adjustment is performed by sending a fixed-intensity light pulse to the SiPMs and scanning through a range of possible switching values. For each setting, the system records whether signals are captured using high or low gain. The ideal point is identified when the transition from high to low gain occurs approximately at the calibrated output corresponding to 20 photoelectrons. This process is repeated for every channel, so each one is tuned individually for maximum accuracy.

With this approach, the readout system preserves maximum resolution for small signals while reliably protecting against distortion from larger pulses, resulting in accurate measurements across the full expected range of input signals.

## 8. Summary and Conclusions

The silicon photomultiplier (SiPM) arrays and BETA-16 ASIC readout system for the FIT tracker have been thoroughly characterized and calibrated using a dedicated laboratory setup. All critical parameters—including timing, trigger thresholds, and multi-stage gain calibration—have been systematically optimized for reliable, high-precision measurements.

A wide dynamic range has been achieved, covering signals from single photoelectrons, such as those produced by minimum ionizing particles, up to the large amplitudes expected from heavy nuclei like iron. Automatic gain switching, tuned using these calibrations, ensures that weak signals are measured with maximum resolution, while strong signals are captured without risk of saturation.

Trigger thresholds have been carefully set under dark conditions, enabling sensitive and stable detection of low-energy events. The full system was validated both in the laboratory and at CERN test beams, and further validation will be carried out in upcoming test beam campaigns.

Overall, the FIT tracker readout is robust, consistent, and fully space-ready for deployment in upcoming missions.

## Acknowledgments

This work is supported by the Spanish Agencia Estatal de Investigación, Ministerio de Ciencia e Innovación: PID2020-116075GB-C22/AEI/10.13039/501100011033, and the FSE+ under the program Ayudas predoctorales of the Ministerio de Ciencia e Innovación PRE2021-097518; European Union NextGenerationEU: PRTR-C17.11; Generalitat de Catalunya; Swiss National Science Foundation (SNSF-PZ00P2 193523).

## References

- [1] S. Maldera *et al.*, “Performance of the Fermi-LAT silicon strip tracker after 14 years of operation,” *Nucl. Instrum. Methods Phys. Res. A* **1049**, 168080 (2023), doi:10.1016/j.nima.2023.168080.
- [2] C. Perrina *et al.*, “Design and Performance of MiniFIT, the small-scale version of the HERD particle tracker,” *PoS* **476**, 06942 (2024), doi:10.22323/1.476.06942.
- [3] A. Sanmukh *et al.*, “Low-power SiPM readout BETA ASIC for space applications,” *Nucl. Sci. Tech.* **35**, 59 (2024), doi:10.1007/s41365-024-01419-z.
- [4] P. Eckert, H.-C. Schultz-Coulon, W. Shen, R. Stamen, and A. Tadday, “Characterisation studies of silicon photomultipliers,” *Nucl. Instrum. Methods Phys. Res. A* **620**, 217–226 (2010), doi:10.1016/j.nima.2010.03.169, arXiv:1003.6071 [physics.ins-det].